

Synthesis and Structural Studies of the A-Site Substituted Bismuth Double Perovskites, $\text{Ba}_{2-x}\text{Sr}_x\text{LuBiO}_6$

Rene B. Macquart and Brendan J. Kennedy*

Centre for Structural Chemistry and Biology, School of Chemistry, The University of Sydney,
Sydney, New South Wales, 2006 Australia

Received August 8, 2004. Revised Manuscript Received February 3, 2005

Seventeen members of the solid solution series $\text{Ba}_{2-x}\text{Sr}_x\text{LuBiO}_6$ have been prepared, and their crystal structures were studied using a combination of powder synchrotron X-ray and neutron diffraction methods. The oxides all adopt a double perovskite-type $\text{A}_2\text{BB}'\text{O}_6$ ($\text{A} = \text{Ba}, \text{Sr}$; $\text{B} = \text{Lu}$, $\text{B}' = \text{Bi}$) structure as a consequence of ordering of the Lu^{3+} and Bi^{5+} cations. As the average ionic radius of the A-site cations (Ba/Sr) decreases the LuO_6 and BiO_6 polyhedra tilt and the structure changes from cubic $Fm\bar{3}m$ ($0 < x < 0.375$) through monoclinic $I2/m$ ($0.375 < x < 1.0$) to monoclinic $P2_1/n$ ($1.0 < x < 2.0$)

Introduction

Perovskite oxides display an array of fascinating magnetic and electrical properties and are arguably the most widely studied class of materials in solid-state chemistry and physics.¹ The term perovskite can be used to describe any material that contains a structural motif similar to that of the mineral perovskite, CaTiO_3 . The importance of perovskite-like phases in the earth's mantle has also prompted considerable interest from the earth-sciences community.¹ While much of the interest in perovskites remains curiosity driven, perovskite related oxides are of considerable commercial importance in a number of fields including piezoelectrics and capacitors. The enormous array of properties displayed by perovskites is linked to the compositional flexibility of the perovskite structure.

The ability of many oxides to retain the basic perovskite structure upon chemical substitutions, including nonstoichiometric substitutions, allows for tuning of the desirable physical properties. Such substitutions can result in, sometimes subtle, structural distortions such as octahedral tilting or ion ordering. Precise structural studies are then required to unravel the complex structure–composition–property relationships in these oxides. This was elegantly demonstrated by Pei and co-workers² in their studies of doped BaBiO_3 .

The discovery of superconductivity in doped BaBiO_3 ^{3–5} prompted numerous studies and it is now well established that this compound contains both Bi^{3+} and Bi^{5+} and that these

have a rock-salt-like ordering in a perovskite type framework.^{2,6,7} The material is best described as $\text{Ba}_2\text{Bi}^{3+}\text{Bi}^{5+}\text{O}_6$ highlighting that this has a double perovskite-type structure. Powder neutron diffraction studies have demonstrated that the average $\text{Bi}^{5+}\text{—O}$ bond distance is noticeably shorter than the average $\text{Bi}^{3+}\text{—O}$ distance: 2.131 vs 2.270 Å.^{2,6,7} At room temperature the Bi charge disproportionation and ordering, coupled with tilting of the BiO_6 octahedra, gives rise to a monoclinic cell, which is described in $I2/m$, the second setting of space group $C2/m$. Heating BaBiO_3 to above ca. 405 K results in a transition to a rhombohedral structure in $R\bar{3}$.^{2,6} Both the monoclinic and rhombohedral structures have only out-of-phase tilting of the octahedra. At still higher temperatures BaBiO_3 becomes cubic, although the charge disproportionation and ordering of the Bi^{5+} and Bi^{3+} cations persists. At low temperatures a primitive monoclinic structure is believed to exist.²

Whereas there are a number of examples of $\text{A}_{1-x}\text{A}'_x\text{BO}_3$ perovskites that, upon variation in the A-site cation, display the same sequence of phases as is observed in variable temperature studies,^{8–12} much less is known about the influence of A-site substitutions on the structures of double perovskites. Considering the temperature-dependent phases in $\text{Ba}_2\text{Bi}^{3+}\text{Bi}^{5+}\text{O}_6$ it is interesting to note that $\text{Sr}_2\text{LuBiO}_6$ has been shown¹³ to be monoclinic at room temperature (Glazer¹⁴ tilt system $a^-a^-c^+$), whereas $\text{Ba}_2\text{LuBiO}_6$ is cubic¹⁵ ($a^0a^0a^0$).

* To whom correspondence should be addressed. E-mail: b.kennedy@chem.usyd.edu.au.

- (1) Mitchell, R. H. *Perovskites: Modern and Ancient*; Almaz Press: Thunder Bay, ON, 2002.
- (2) Pei, S.; Jorgensen, J. D.; Dabrowski, B.; Hinks, D. G.; Richards, D. R.; Mitchell, A. W.; Newsam, J. M.; Sinha, S. K.; Vaknin, D.; Jacobson, A. J. *Phys. Rev., B* **1990**, *41*, 4126.
- (3) Cava, R. J.; Batlogg, B.; Krajewski, J. J.; Farrow, R. C.; Rupp, L. W., Jr.; White, A. E.; Short, K. T.; Peck, W. F., Jr.; Kometani, T. Y. *Nature* **1988**, *332*, 814.
- (4) Sleight, A. W.; Gillson, J. L.; Bierstedt, P. E. *Solid State Commun.* **1975**, *17*, 27.
- (5) Uchida, S.; Kitazawa, K.; Tanaka, S. *Phase Transitions* **1987**, *8*, 95.

- (6) Thornton, G.; Jacobson, A. J. *Acta Crystallogr. B* **1978**, *34*, 351.
- (7) Cox, D. E.; Sleight, A. W. *Solid State Commun.* **1976**, *19*, 969. See also Cox, D. E.; Sleight, A. W. *Acta Crystallogr. B* **1979**, *35*, 1.
- (8) Ball, C. J.; Begg, B. D.; Cookson, D. J.; Thorogood, G. J.; Vance, E. R. *J. Solid State Chem.* **1998**, *139*, 238.
- (9) Kennedy, B. J.; Howard, C. J.; Chakoumakos, B. C. *J. Phys.: Condens. Matter* **1999**, *11*, 1479.
- (10) Howard, C. J.; Knight, K. S.; Kennedy, B. J.; Kisi, E. H. *J. Phys.: Condens. Matter* **2000**, *12*, L677.
- (11) Kennedy, B. J.; Howard, C. J.; Thorogood, G. J.; Hester, J. R. *J. Solid State Chem.* **2001**, *161*, 106.
- (12) Li, L.; Kennedy, B. J.; Kubota, Y.; Kato, K.; Garrett, R. F. *J. Mater. Chem.* **2004**, *14*, 263.
- (13) Harrison, W. T. A.; Reis, K. P.; Jacobson, A. J.; Schneemeyer, L. F.; Waszczak, J. V. *Chem. Mater.* **1995**, *7*, 2161.
- (14) Glazer, A. M. *Acta Crystallogr., B* **1972**, *28*, 3384. Glazer, A. M. *Acta Crystallogr., A* **1975**, *31*, 756.

This situation is similar to that seen in $AZrO_3$ where the Sr compound is orthorhombic ($a^-a^+c^+$) and the Ba compound is cubic ($a^0a^0a^0$). Importantly, the same sequence of phases, $Pnma \rightarrow \{Imma \rightarrow I4/mcm \rightarrow Pm\bar{3}m\}$ is seen in the solid solutions $Sr_{1-x}Ba_xZrO_3$ ¹¹ as is observed in $SrZrO_3$ at elevated temperatures.¹⁰ There have been no structural studies of the solid solutions between Sr_2LuBiO_6 and Ba_2LuBiO_6 . If the composition-driven phase transformations in the double perovskites mimics those induced by temperature changes then a series of intermediate phases is expected in the $Ba_{2-x}Sr_xLuBiO_6$ solid solutions as the structure changes from one with no tilts to one with three tilts. The present work describes the preparation and structures of such solid solutions.

Experimental Section

The crystalline samples of $Ba_{2-x}Sr_xLuBiO_6$ were prepared by the solid-state reaction of stoichiometric quantities of Bi_2O_3 (99.999%, Aldrich), Lu_2O_3 (99.99% Aldrich), $BaCO_3$ (99.9%, Aldrich), and $SrCO_3$ (99.9%, Aldrich). The powders were first mixed together and ground to a uniform slurry under acetone in an agate mortar, they were then placed into uncovered alumina crucibles. The heating sequence used was 800 °C/24 h, 900 °C/24 h, 1000 °C/120 h, and 1050 °C/48 h with intermediate regrinding. The samples, ranging in color from a light tan to a dark brown, were slowly cooled to room temperature in the furnace.

The sample purity was established by powder X-ray diffraction measurements using Cu K α radiation on a Shimadzu D-6000 Diffractometer. Synchrotron X-ray powder diffraction patterns were collected on the high-resolution Debye Scherrer diffractometer at beamline 20B, the Australian National Beamline Facility, at the Photon Factory, Japan.¹⁶ The samples were finely ground and loaded into 0.3-mm glass capillaries that were rotated during the measurements. All measurements were performed under vacuum to minimize air scatter. Data were recorded using two Fuji image plates. Each image plate was 20 × 40 cm and covered 40° in 2 θ . A thin strip ca. 0.5 cm wide was used to record each diffraction pattern so that up to 30 patterns could be recorded before reading the image plates. The data were collected at a wavelength of 0.80282 Å (calibrated with a NIST Si 640c standard) over the 2 θ range of 5–85° with step size of 0.01°.

Neutron powder diffraction data were collected at the HIFAR facility operated by the Australian Nuclear Science and Technology Organization (ANSTO) using the high-resolution powder diffractometer at a wavelength of 1.4928 Å.¹⁷ Each sample was held in an aluminum-capped vanadium sample holder and was rotated throughout the measurements. The diffractometer is equipped with 24 ³He detectors individually separated by 5°. The patterns were collected at room temperature over the 2 θ range 5–150° with step size of 0.05°. Structures were refined by the Rietveld method using the program Rietica.¹⁸ The diffraction peaks were described by a pseudo-Voigt function where the Lorentzian fraction is refined. For the neutron diffraction studies a correction for peak asymmetry was made for angles below 35° in 2 θ . The background was described by a six-parameter polynomial. For the X-ray profiles the background was estimated by interpolation between up to 40 user selected points.

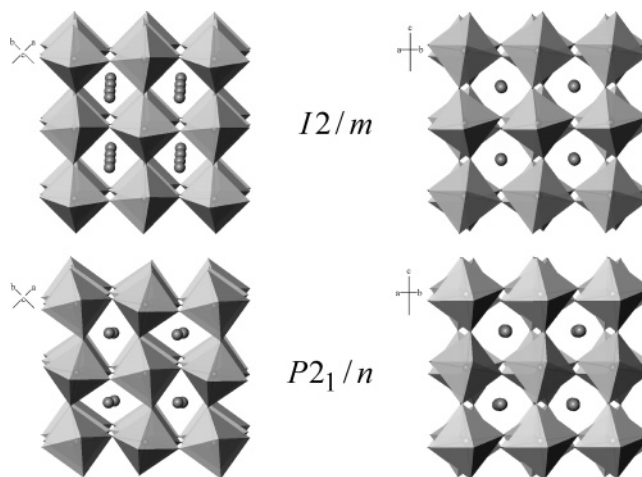


Figure 1. Representation of the two monoclinic structures observed in the series $Ba_{2-x}Sr_xLuBiO_6$. The left images show the in-phase tilt about the [001] axis to be present in $P2_1/n$ but absent in $I2/m$, whereas, as seen in the right side images, the out-of-phase tilt about the [110] axis is apparent in both phases. The small spheres represent the A-type cations.

Results and Discussion

The X-ray patterns for all 17 samples appeared indicative of single-phase perovskite-like materials. In all cases a number of odd–odd–odd reflections diagnostic of a rock-salt-like ordering of the Lu and Bi cations were observed, as shown in Figure 1.¹⁹ This ordering is induced primarily by the charge difference between the Lu^{3+} and Bi^{5+} cations, with the size of these two cations being reasonably similar: 0.86 and 0.76 Å. Bi^{3+} is noticeably larger than either of these, at 1.03 Å.²⁰ The powder pattern of Ba_2LuBiO_6 was indexed to a $Fm\bar{3}m$ cubic cell with unit cell parameter $a = 8.5154(1)$ Å. The observed cubic lattice parameter is approximately double that observed in simple ABO_3 perovskites as a consequence of the ordering of the Lu and Bi cations. The pattern for Sr_2LuBiO_6 was indexed to a $P2_1/n$ monoclinic cell with $a = 5.85833(7)$ Å, $b = 5.92541(7)$ Å, $c = 8.32188(11)$ Å, and $\beta = 90.085(1)^\circ$. The cell can be described as having a $\sqrt{2}a_p \times \sqrt{2}a_p \times 2a_p$ super structure of a primitive-cubic parent perovskite that has a cell length, a_p , ≈ 4.2 Å (Figure 1). These results are in excellent agreement with previously reported values.^{13,15} For Sr_2LuBiO_6 the superstructure arises from the combination of cation ordering and tilting of the octahedra, the latter being described in the notation of Glazer¹⁴ as $a^-a^-c^+$; that is, out-of-phase tilting occurs about the $[100]_p$ and $[010]_p$ pseudocubic axes and in-phase tilting occurs about the $[001]_p$ axis. This change in symmetry from cubic $x = 0$ to monoclinic $x = 2$ in the series $Ba_{2-x}Sr_xLuBiO_6$ is in keeping with the change in the effective size of cation at the A-type sites. The tilting of the BO_6 octahedra arises because of the poor geometrical fit of the smaller Sr cations into the A-site.

The synchrotron diffraction patterns showed the structures to remain cubic with increasing Sr content until $x \approx 0.375$.

(15) Wolcyrz, M.; Kepinski, L. *J. Alloys Compd.* **1999**, 287, 137.

(16) Sabine, T. M.; Kennedy, B. J.; Garrett, R. F.; Foran, G. J.; Cookson, D. J. *J. Appl. Crystallogr.* **1995**, 28, 513.

(17) Howard, C. J.; Ball, C. J.; Davis, R. L.; Elcombe, M. M. *Aust. J. Phys.* **1983**, 36, 507.

(18) Howard, C. J.; Hunter, B. A. *A Computer Program for Rietveld Analysis of X-ray and Neutron Powder Diffraction Patterns*; Lucas Heights Research Laboratories: NSW, Australia, 1998; pp 1–27.

(19) Howard, C. J.; Kennedy, B. J.; Woodward, P. W. *Acta Crystallogr. B* **2004**, 59, 463.

(20) Shannon, R. D. *Acta Crystallogr. A* **1976**, 32, 751.

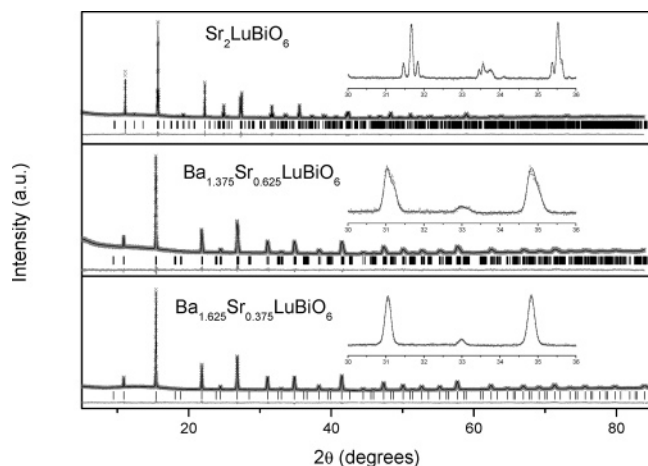


Figure 2. Representative examples of the synchrotron X-ray diffraction profiles. $\text{Ba}_{1.625}\text{Sr}_{0.375}\text{LuBiO}_6$ has cubic symmetry in $Fm\bar{3}m$, $\text{Ba}_{1.375}\text{Sr}_{0.625}\text{LuBiO}_6$ has monoclinic symmetry in $I2/m$, and $\text{Sr}_2\text{LuBiO}_6$ has monoclinic symmetry in $P2_1/n$. The solid lines are the fits obtained by the Rietveld method to the parameters listed in Table 3.

At this point there appeared to be an abrupt change in the appearance of the diffraction patterns. On the assumption that the change in symmetry is a consequence of the rotation of the BO_6 octahedra we considered it unlikely that all three tilts of the monoclinic $P2_1/n$ structure would appear simultaneously and that a series of intermediate phases may be expected. By inspection of Figure 1 of the work of Howard, Kennedy, and Woodward¹⁹ we identified a number of possible intermediate phases. Analysis of the observed peak splitting and systematic absences suggested the most appropriate structure was monoclinic in $I2/m$, which has an $a^0b^-b^-$ Glazer tilt system. For example, the (cubic) 220 reflection near $2\theta = 15^\circ$ is observed to split into three well resolved peaks in the monoclinic structure: the 020, 112 and 200 reflections. The primitive 113 reflection that is clearly observed in $\text{Sr}_2\text{LuBiO}_6$ near $2\theta = 20^\circ$ is not observed in these monoclinic cells. We note that a $Fm\bar{3}m$ to $I2/m$ transition is required to be first order,¹⁹ therefore an abrupt change between these is not surprising. What is somewhat surprising is that we see no evidence for an intermediate phase, in particular the rhombohedral $R\bar{3}$ phase.

The $I2/m$ structure can be described in terms of the same $\sqrt{2}a_p \times \sqrt{2}a_p \times 2a_p$ superstructure as the more commonly observed $P2_1/n$ structure^{21,22} and differs mainly by the absence of the in-phase tilts. As evident from Figure 2 the I -centered monoclinic cell does not contain any reflections that cannot be indexed to the same cell as the F -centered cubic cell, although the lowering of symmetry results in the splitting of a number of reflections. The absence of any additional reflections in the monoclinic cell arises since both the rock-salt-like cation ordering and the out-of-phase tilting of the BO_6 octahedra are associated with the same R-point mode.

At around $x = 1.0$ a number of very weak reflections with hkl ; $h + k + l \neq 2n$ indicative of a primitive cell were observed. These became progressively stronger as the Sr

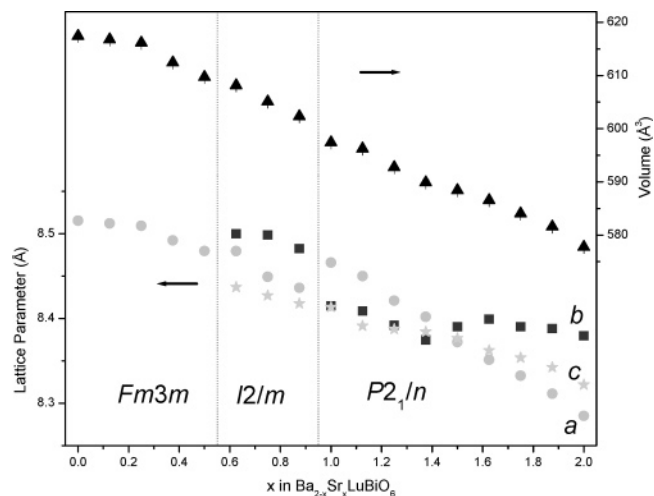


Figure 3. Composition-dependence of the lattice parameters (lower section) and volume in the series $\text{Ba}_{2-x}\text{Sr}_x\text{LuBiO}_6$. The dashed vertical lines show the approximate transition points for the three structures. Note that there is a change in axes directions between the two monoclinic structures. For ease of comparison the a - and b -lattice parameters in the monoclinic structures have been multiplied by $\sqrt{2}$.

content increased. Such reflections are associated with a M_3^+ mode that corresponds to in-phase tilting of octahedra in successive layers. The splitting of the stronger reflections did not show any appreciable variation near this composition and these peaks could be indexed on the same size monoclinic cell. This shows that near $x = 1$ the structure transforms from one in $I2/m$ to one in $P2_1/n$. The structures were then refined using the synchrotron diffraction data using the composition limits $P2_1/n \xrightarrow{x=1} I2/m \xrightarrow{x=0.375} Fm\bar{3}m$. Representative examples of the refinements are shown in Figure 2 and the composition dependence of the lattice parameters and volumes is illustrated in Figure 3. As noted above the $I2/m$ to $Fm\bar{3}m$ transition must be first order, however the $P2_1/n$ to $I2/m$ transition can be continuous¹⁹ and we see nothing from the variation in lattice parameters to suggest this is not the case.

During the refinements we observed a number of weak broad features in the difference profiles of several samples that could be indexed on the basis of a primitive cubic cell with $a \approx 4.25$ Å. It appears that some of the samples contained a small amount of a disordered cubic perovskite-like phase; this appears to represent around 5 wt % of the sample and has a composition similar to that of the bulk phase. This effect has been observed in other complex oxides.²³ The inclusion of such a second phase in the refinements improved the refinement statistics but otherwise did not alter either the refined lattice parameters or atomic coordinates.

In all cases the refined displacement parameters were physically reasonable and attempts to refine anti-site disorder between the Bi and Lu cations suggested that negligible site mixing occurred. In the final refinement cycles full ordering of the Bi and Lu was assumed. In their study of the series of rare-earth-containing oxides $\text{Ba}_2\text{LnBiO}_6$ Harrison and co-workers¹³ concluded that disorder only occurred where the

(21) Anderson, M. T.; Greenwood, K. B.; Taylor, G. A.; Poeppelmeier, K. R. *Prog. Solid State Chem.* **1993**, 22, 197.

(22) Woodward, P. M. *Acta Crystallogr. B* **1997**, 53, 44.

(23) Bieringer, M.; Moussa, S. M.; Noailles, L. D.; Burrows, A.; Kiely, C. J.; Rosseinsky, M. J.; Ibberson, R. M. *Chem. Mater.* **2003**, 15, 586.

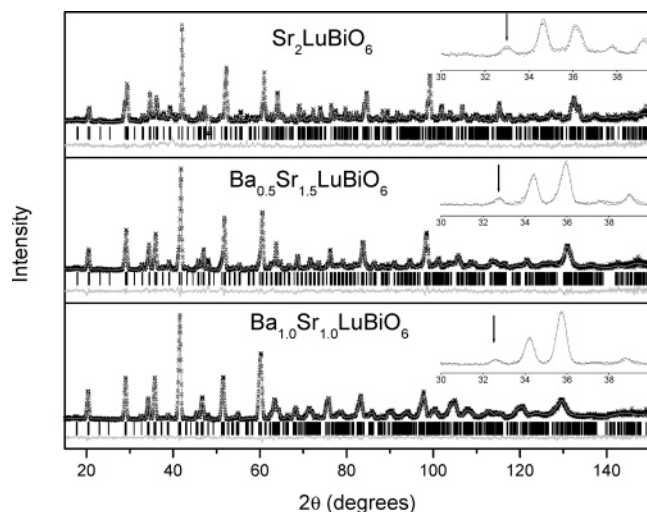


Figure 4. Rietveld neutron refinement profiles for the monoclinic $P2_1/n$ monoclinic structures in the series $Ba_{2-x}Sr_xLuBiO_6$. The inserts highlight the gradual loss of intensity in the selected reflections as the magnitude of the out-of-phase tilting decreases with increasing Ba content. The 210/120 pair is indicated by the arrow. The structural parameters are listed in Table 1.

RE cation had a chemically accessible M^{4+} oxidation state (RE = Ce, Pr, Tb). The present results are consistent with this conclusion.

Although the structural refinements were apparently successful, the refined bond distances showed a large amount of scatter and there did not appear to be any systematic variation in these. In general the average Lu–O and Bi–O bond distances were approximately equal, but the Bi–O distances were not always smaller than the Lu–O distances as would be expected from the differences in the ionic radii of Bi^{5+} (0.76 Å) and Lu^{3+} (0.86 Å). For example in $Ba_{1.625}Sr_{0.375}LuBiO_6$, Bi–O was 2.16(4) Å and Lu–O was 2.10(4) Å. Consequently, the structures of three representative examples were refined using powder neutron diffraction data.

The powder neutron diffraction profile for Sr_2LuBiO_6 shows a number of relatively strong primitive reflections indicative of in-phase tilting of the octahedra. These are most obvious in Figure 4 in the region just below 40° . As evident from Figure 4 as the Ba content was increased, these noticeably weakened. During the refinement of the structure of Sr_2LuBiO_6 a number of weak additional peaks due to the aluminum caps on the vanadium sample holder were observed. The regions most affected were excluded from the refinements. The refined atomic positional parameters for Sr_2LuBiO_6 are listed in Table 1. This model also proved adequate for both the $x = 0.5$ and 1.0 samples (Table 1).

The refinements using the neutron diffraction data confirm that although the Lu–O and Bi–O distances are similar the refined Bi–O distances are systematically smaller (Table 2), and the volume of the BiO_6 octahedra is around 5% larger (12.7 Å³) in Sr_2LuBiO_6 cf. 12.0 Å³ for the LuO_6 octahedra. In addition to providing a more accurate measure of the various bond distances, the refined atomic coordinates were used to calculate the magnitude of the tilts about the [001] (φ) and [110] (θ) axes of the cubic aristotype as described by Groen.²⁴ We observe (Table 2) the magnitude of the tilt about the [001] axis to be smaller than that about the 110

Table 1. Refined Structural Parameters for Monoclinic $P2_1/n$ Phases in the Series $Ba_{2-x}Sr_xLuBiO_6$ ^a

atom	x	y	z	B (Å ²)
Sr_2LuBiO_6^b				
Sr	0.9920(11)	0.4643(5)	0.2543(16)	0.8(1)
Lu	0	0	1/2	0.5(2)
Bi	0	0	0	0.6(2)
O1	0.0845(10)	0.0243(10)	0.2548(18)	1.2(1)
O2	0.2134(21)	0.2984(17)	−0.0410(14)	1.2(2)
O3	0.2973(18)	0.7846(19)	−0.0460(15)	0.8(2)
$Ba_{0.5}Sr_{1.5}LuBiO_6$^c				
Sr/Ba	0.9856(19)	0.4729(9)	0.2514(28)	0.7(1)
Lu	0	0	1/2	0.2(2)
Bi	0	0	0	0.7(3)
O1	0.0756(16)	0.0191(12)	0.2430(16)	0.5(1)
O2	0.2201(28)	0.2763(37)	−0.0341(17)	1.2(3)
O3	0.2928(27)	0.7881(22)	−0.0412(16)	1.0(3)
$BaSrLuBiO_6$^d				
Sr/Ba	0.9800(24)	0.4856(13)	0.2415(14)	0.6(1)
Lu	0	0	1/2	0.4(2)
Bi	0	0	0	0.7(2)
O1	0.0727(10)	0.0130(13)	0.2451(11)	0.1(1)
O2	0.2411(21)	0.2711(18)	−0.0219(13)	1.4(2)
O3	0.2909(18)	0.7864(20)	−0.0298(12)	1.1(2)

^a The structural refinements used powder neutron diffraction data. Numbers in parentheses are estimated standard deviations of the last significant figure, and in the case of the lattice parameters neglect the uncertainty in the neutron wavelength. Where no standard deviation is given, the parameter was not refined. ^b $a = 5.8558(4)$ Å; $b = 5.9232(5)$ Å; $c = 8.3194(7)$ Å; $\beta = 90.068(7)^\circ$. R_p 6.06; R_{wp} 7.63; χ^2 2.41%. ^c $a = 5.9128(9)$ Å; $b = 5.388(10)$ Å; $c = 8.3702(18)$ Å; $\beta = 90.187(18)^\circ$. R_p 6.48; R_{wp} 8.07; χ^2 2.30%. ^d $a = 5.9440(8)$ Å; $b = 5.9433(7)$ Å; $c = 8.4519(11)$ Å; $\beta = 90.426(10)^\circ$. R_p 6.07; R_{wp} 7.46; χ^2 1.91%.

Table 2. Selected Bond Distances and Tilt Angles Obtained from Refinements Using Neutron Diffraction Data^a

bond	Sr_2LuBiO_6	$Sr_{1.5}Ba_{0.5}LuBiO_6$	$SrBaLuBiO_6$
Lu–O(1) Å	2.163(9)	2.096(14)	2.120(16)
Lu–O(2) Å	2.159(8)	2.154(15)	2.166(11)
Lu–O(3) Å	2.178(13)	2.196(15)	2.159(10)
Lu–O (avg)	2.167	2.149	2.148
θ°	13.4	12.0	11.5
φ°	9.5	7.8	6.0
Bi–O(1) Å	2.119(9)	2.190(15)	2.197(16)
Bi–O(2) Å	2.135(9)	2.100(16)	2.063(11)
Bi–O(3) Å	2.108(13)	2.105(16)	2.112(11)
Bi–O (avg)	2.121	2.131	2.124
θ°	14.1	12.7	12.0
φ°	9.6	8.0	6.3

^a The tilt about the cubic, 4-fold axis is given by φ and that about the 2-fold axis is given by θ .

axis and this appears to be approaching zero near $x = 1$. In $I2/m$ this angle is required to be equal to zero. Conversely the tilt about the 2-fold [110] axis remains well above zero even in $BaSrLuBiO_6$ (Table 2). This tilt is nonzero in $I2/m$. In general, the magnitude of the tilts about the two types of cations is similar, as expected, given the similarity in their ionic radii.

It is interesting to note the absence of an intermediate rhombohedral phase in the series $Ba_{2-x}Sr_xLuBiO_6$. It appears that the composition-induced transformation proceeds directly from $Fm\bar{3}m$ to $I2/m$. A rhombohedral phase was observed in a single sample in the series Ba_2LnBiO_6 by Harrison et al.²⁴ for $Ln = Yb$. Ba_2ErBiO_6 is monoclinic in $I2/m$ (ionic radius of Er^{3+} is 0.890 Å) whereas Ba_2LuBiO_6 is cubic (Lu^{3+} , 0.861 Å). The ionic radius of Yb^{3+} , 0.868 Å, is intermediate

(24) Groen, W. A.; Van Berkel, F. P. F.; Ijdo, D. J. W. *Acta Crystallogr. C* **1986**, 42, 1472.

Table 3. Representative Examples of Refined Structural Parameters Using Synchrotron Diffraction Data in Each of the Three Space Groups Observed in the Series $\text{Ba}_{2-x}\text{Sr}_x\text{LuBiO}_6$

atom	site	x	y	z
$\text{Sr}_2\text{LuBiO}_6$; Space Group $P2_1/n$^a				
Sr	4e	0.9947(17)	0.4634(4)	0.2501(19)
Bi	2a	0	0	0
Lu	2b	0	0	1/2
O1	4e	0.0718(24)	0.0183(33)	0.2497(36)
O2	4e	0.1917(39)	0.2818(51)	-0.0485(35)
O3	4e	0.2586(49)	0.7930(44)	-0.0437(34)
$\text{Ba}_{1.375}\text{Sr}_{0.625}\text{LuBiO}_6$; Space Group $I2/m$^b				
Sr	4i	0.5016(22)	0	0.2507(18)
Bi	2a	0	0	0
Lu	2d	0	0	1/2
O1	4i	0.0740(53)	0	0.2427(39)
O2	8j	0.2578(32)	0.7603(44)	-0.0389(15)
$\text{Ba}_{1.625}\text{Sr}_{0.375}\text{LuBiO}_6$; Space Group $Fm\bar{3}m$^c				
Ba	8c	1/4	1/4	1/4
Bi	4b	1/2	1/2	1/2
Lu	4a	0	0	0
O1	24e	0.2510(47)	0	0

^a $a = 5.85833(7)$ Å; $b = 5.92541(7)$ Å; $c = 8.32188(11)$ Å; $\beta = 90.085(1)^\circ$; R_p 4.54; R_{wp} 5.76%. ^b $a = 5.9956(4)$ Å; $b = 6.0104(4)$ Å; $c = 8.4367(4)$ Å; $\beta = 90.468(3)^\circ$; R_p 4.70; R_{wp} 5.95%. ^c $a = 8.4922(1)$ Å; R_p 3.39; R_{wp} 4.32%.

between these two extremes.²⁰ Apparently small changes in the size of the trivalent rare earth cation are sufficient to destabilize this rhombohedral structure. The structure of the rhombohedral phase in $\text{Ba}_2\text{YbBiO}_6$ is the same as observed in $\text{Ba}_2\text{Bi}^{3+}\text{Bi}^{5+}\text{O}_6$,^{5,6} at high temperatures where it is intermediate between the room-temperature monoclinic $I2/m$ and high-temperature cubic $Fm\bar{3}m$ structures. This rhombohedral phase has also been found to be present in other Bi containing double perovskites including $\text{Ba}_2\text{TaBiO}_6$ ²⁵ and $\text{Ba}_2\text{SbBiO}_6$.²⁶ It is possible that such a rhombohedral phase exists over a very small composition range in the series $\text{Ba}_{2-x}\text{Sr}_x\text{LuBiO}_6$.

The stability of the cubic perovskite structure is often estimated using the Goldschmidt tolerance factor, t , defined as $t = r_A + r_O/\sqrt{2}(r_B + r_O)$ where r_O is the ionic radius of the oxygen anion and r_A and r_B are the effective ionic radii of the cations on the A and B sites, respectively. For double perovskites Teraoka²⁷ has suggested a more sensitive function is $\phi = \sqrt{2}r_A/(r_B + r_O)$ and postulated that cubic structures

are favored when $\phi > 1.00$ and monoclinic structures in $P2_1/n$ are favored when $\phi < 0.90$. Intermediate values of ϕ correspond to other symmetries. Our results apparently agree with these conclusions: ϕ for $\text{Ba}_2\text{LuBiO}_6$ is 1.030 and for $\text{Sr}_2\text{LuBiO}_6$ it is 0.894. Further, ϕ becomes equal to 1.00 near $x = 0.276$ which is in fair agreement with the position of the composition-induced transformation from the cubic structure. However, this relationship, like the tolerance factor, is not sufficiently precise to predict the precise symmetry since ϕ varies in the series $\text{Ba}_2\text{LnBiO}_6$ (Ln = Er, Yb, and Lu) as 1.023, 1.027, and 1.030 corresponding to the observed sequence of symmetries $I2/m \rightarrow R\bar{3} \rightarrow Fm\bar{3}m$. At the same time $\text{Ba}_2\text{Bi}^{3+}\text{Sb}^{5+}\text{O}_6$ has $\phi = 1.028$ and is monoclinic ($I2/m$) at room temperature.

Conclusion

The series of A-site substituted bismuth double perovskites, $\text{Ba}_{2-x}\text{Sr}_x\text{LuBiO}_6$ has been synthesized at ambient pressure using conventional solid-state methods, and their structures were determined from high-resolution powder synchrotron X-ray diffraction data. Structures were refined using the Rietveld method, in some cases using neutron diffraction data. In all cases the Lu and Bi cations were ordered into alternate octahedra. The structures of the Ba rich oxides with $x \leq 0.375$ were found to be cubic in $Fm\bar{3}m$ and the Sr rich oxides with $x \geq 1$ were monoclinic in $P2_1/n$. At intermediate compositions the structures were also monoclinic but in $I2/m$. These changes in symmetry are a consequence of tilting of the BO_6 octahedra. We did not observe any evidence for a rhombohedral intermediate phase.

Acknowledgment. The work performed at the Australian National Beamline Facility was supported by the Australian Synchrotron Research Program, which is funded by the Commonwealth of Australia under the Major National Research Facilities program. The Australian Institute of Nuclear Science and Engineering supported the neutron diffraction experiments. B.J.K. acknowledges the support of the Australian Research Council. The assistance of Dr. James Hester at the ANBF and Dr. Margaret Elcombe at ANSTO is gratefully acknowledged.

CM0486924

(25) Fu, W. T. *Solid State Commun.* **2000**, *116*, 461.

(26) Zhou, Q.; Kennedy, B. J. Unpublished work.

(27) Teraoka, Y.; Wei, M. D.; Kagawa, S. *J. Mater Chem.* **1978**, *8*, 2323.